Techno-economic analysis and optimisation of grey and green methanol synthesis using flowsheet automation and surrogate modelling

Anders Andreasen*,† and Jasper van Baten‡

†*Process Department, Energy Transition, Ramboll Energy, Bavnehøjvej 5, Esbjerg, DK-6700, Denmark*

‡*AmsterCHEM, Calle Las Rozas 32, 04618 Las Rozas / Cuevas del Almanzora, Almería, Spain*

E-mail: anra@ramboll.com

Abstract

Recognizing methanol's versatile role as a chemical precursor and energy carrier, the study addresses its traditional production from fossil fuels and the associated challenges in pivoting to green alternatives due to the cost of green hydrogen. The research focuses on techno-economic analysis and optimization, employing a validated chemical process simulation tool integrated with economic analyses, reflecting CAPEX and OPEX models, and considering heat recovery to promote self-sufficiency. The study compares grey (traditional syngas) and green (biogenic CO_2 and green hydrogen) methanol production pathways while also optimizing process factors, such as feed pressure, purge rate, temperature and catalyst volume, to achieve cost-effectiveness.

In green methanol production specifically, the paper finds that optimal conditions are slightly milder than for grey methanol, highlighting the importance of process variables like purge rate given the high cost of green hydrogen. Still with current price

level of hydrogen from electrolysis the levelised cost of methanol is several times more expensive via direct hydrogenation compared to production from fossil syngas. Results from the simulation-driven optimization underline the delicate balance between various objectives, such as minimizing costs or maximizing output, and demonstrate instances of pareto optimality.

This study thus contributes with an integrated assessment of methanol production techniques, utilizing process simulation, economic evaluation, and heat integration for both grey and green methanol, aiming to pave the way for more sustainable chemical processes in the industry.

Nomenclature

A Area

ACHE Air Cooled Heat Exchanger

API American Petroleum Institute

ASME American Society of Mechanical Engineers

BM Bare Module

BPVC Boiler and Pressure Vessel Code

CAPEX Capital Expenditure

CEPCI Chemical Engineering Plant Cost Index

CF Capacity factor

COCO CAPE-OPEN to CAPE-OPEN

COFE CAPE-OPEN Flowsheet Environment

COM Component Object Model

CRF Capital Recovery Factor

CS Carbon Steel

DACE DEsign and Analysis of Computer Experiements

DE Differntial Evolution

DIRECT DIviding RECTangles

DME Dimethyl ether

DOE (U.S.) Department of Energy

DoE Design of Experiements

EPC Engineering Procurement Construction

FEED Front End Engineering Design

FOB Free On-Board

FOPEX Fixed Operational Expenditure

GHSV Gas Hourly Space Velocity

GPSA Gas Processors Suppliers Association

ISBL Inside battery limit

KDB Korea Thermophysical Properties Data Bank

LCOE Levelised Cost of Energy / Electricity

LCOM Levelised Cost of Methanol

LHS Latin Hybecube Sampling

LMTD Logarithmic Mean Temperature Difference

m Mass

MeOH Methanol

MM Mille Mille

MTBE Methyl tert-butyl ether

MTD Mean Temperature Difference

NETL National Energy Technology Laboratory

NREL National Renewable Energy Laboratory

NRTL Non-Random Two-Liquid (model)

NSGA Non-dominated Sorting Genetic Algorithm

O&M Operations and Maintenance

OEM Original Equipment Manufacturer

OFAT One Factor At Time

OPEX Operational Expenditure

OSBL Outside battery limit

P Power

PM Physical Module

PR Peng-Robinson

RMSE Rott Mean Squared Error

ROI Return Of Investment

RSM Response Surface Methodology

RWGS Reverse Water Gas Shift

SHE Shell & Tube Heat Exchanger

SHGO Simplicial Homology Global Optimization

SLSQP Sequential Least-SQuares Programming

SS Stainless Steel

TM Total Module

TNO Nederlandse organisatie voor toegepast-natuurwetenschappelijk onderzoek

TOTEX Total Expenditure (annualised)

TPC Total Plant Cost

USD U.S. Dollars

VBA Visual Basic for Applications

VF Vapour Fraction

VLE Vapour Liquid Equilibrium

VOPEX Variable Operational Expenditure

Introduction

Methanol is an important and versatile building block in the chemical industry, a precursor to formaldehyde and polymers as well as acetic acid, MTBE and DME etc. Methanol can also be turned into higher hydrocarbons/olefins to name a few usages. It is the basis of a vast amount of everyday products. Further, methanol is an energy carrier and can be used

for fuel blending and as fuel on its own, substituting gasoline and diesel. The use as energy carrier and fuel is still limited, but e.g. larger container vessels have already been built with methanol-ready two-stroke Diesel engines. Methanol production is almost entirely based on fossil fuel, via steam reforming and syngas. For sustainable methanol production, the synthesis of methanol via the direct hydrogenation of biogenic CO_2 using green hydrogen is a promising path. However, the cost of green hydrogen is a challenge that may jeopardise large scale roll-out of green methanol (also termed e-Methanol) production and its widespread adaption.

In lieu of a comprehensive literature review of methanol synthesis itself, both the conventional route from fossil feedstock as well as direct hydrogenation of CO_2 and H_2, the reader is referred to other good comprehensive reviews and overviews such as.[1–6] References with direct relation to the present work will be cited in the appropriate context.

Techno-economic aspects of methanol synthesis has been dealt with by numerous researchers. To name a few, Atsbha *et al.*[7] noted an almost 1:1 effect of the cost of hydrogen on the unit production cost of methanol via direct hydrogenation and Campos *et al.*[8] investigated a three-step direct hydrogenation synthesis process and compared it to a conventional one-step process and found a slight improvement in the techno-economic key performance indicators and also concluded that for green methanol to be competitive with grey methanol the cost of renewable hydrogen should drop below 1.5 USD/kg. Cameli *et al.*[9] conducted a techno-economic analysis of an e-methanol plant using CO_2 from direct air capture and H_2 produced by electrolysis. Optimisation of methanol synthesis from syngas have been investigated by Luyben[10] by a one-factor at a time methodology, by Alarifi *et al.*[11] using a multi-objective optimisation approach for a multi-bed intermediate quenching process.

The justification for the presented work is the obvious need for techno-economic optimisation, especially when it comes to making attempts at green methanol production. To the best of our knowledge most techno-ecomonic analysis of methanol synthesis has been focused on the comparison of different process flow schemes and making sensitivity analysis. Param-

eter optimisation within a predefined process configuration combined with techno-economic analysis is apparently lacking from the literature.

In the present paper, a study is performed focussing on techno-economic analysis and optimisation of both grey (syngas) and green methanol production. The core of this study is centered around a freely available process simulation tool which, after rigorous validation and fidelity establishment, is used to generate training and test sets for surrogate model building, facilitating easy and speedy combination with relevant optimisation algorithms. This is facilitated by a high level of automation via a python wrapper. An economic analysis is built into the wrapper including CAPEX models for all main equipment and corresponding total plant cost as well an OPEX model factoring in both variable and fixed costs. In addition, the importance and implications of various means of heat recovery and heat integration are also addressed in order to make the methanol synthesis process self-supplied with heat.

Methods

Methanol synthesis kinetics and implementation

The kinetic model forming the basis of the present study is the one proposed by Vanden Bussche and Froment.[12] The following two reactions, the direct hydrogenation of CO_2 to methanol (MeOH) and the reverse water gas shift (RWGS) reaction, are considered to adequately describe methanol synthesis from syngas.

$$CO_2 + 3\,H_2 \rightleftharpoons CH_3OH + H_2O \tag{1}$$

$$CO_2 + H_2 \rightleftharpoons CO + H_2O \tag{2}$$

The kinetic expressions for the two reactions can be written as:[12,13]

$$r_{\mathrm{MeOH}} = \frac{k_1 p_{\mathrm{CO_2}} p_{\mathrm{H_2}} \left(1 - \frac{1}{K_{eq1}} \frac{p_{\mathrm{H_2O}} p_{\mathrm{CH_3OH}}}{p_{\mathrm{H_2}}^3 p_{\mathrm{CO_2}}}\right)}{\left(1 + k_2 \frac{p_{\mathrm{H_2O}}}{p_{\mathrm{H_2}}} + k_3 p_{\mathrm{H_2}}^{0.5} + k_4 p_{\mathrm{H_2O}}\right)^3} \tag{3}$$

$$r_{\mathrm{RWGS}} = \frac{k_5 p_{\mathrm{CO_2}} \left(1 - K_{eq2} \frac{p_{\mathrm{H_2O}} p_{\mathrm{CO}}}{p_{\mathrm{H_2}} p_{\mathrm{CO_2}}}\right)}{\left(1 + k_2 \frac{p_{\mathrm{H_2O}}}{p_{\mathrm{H_2}}} + k_3 p_{\mathrm{H_2}}^{0.5} + k_4 p_{\mathrm{H_2O}}\right)} \tag{4}$$

For the implementation in the present work, the rearranged equations as given by Van-Dal and Bouallou[13] are used.

$$r_{\mathrm{MeOH}} = \frac{k_1 p_{\mathrm{CO_2}} p_{\mathrm{H_2}} - k_6 \frac{p_{\mathrm{H_2O}} p_{\mathrm{CH_3OH}}}{p_{\mathrm{H_2}}^2}}{\left(1 + k_2 \frac{p_{\mathrm{H_2O}}}{p_{\mathrm{H_2}}} + k_3 p_{\mathrm{H_2}}^{0.5} + k_4 p_{\mathrm{H_2O}}\right)^3} \tag{5}$$

$$r_{\mathrm{RWGS}} = \frac{k_5 p_{\mathrm{CO_2}} - k_7 \frac{p_{\mathrm{H_2O}} p_{\mathrm{CO}}}{p_{\mathrm{H_2}}}}{\left(1 + k_2 \frac{p_{\mathrm{H_2O}}}{p_{\mathrm{H_2}}} + k_3 p_{\mathrm{H_2}}^{0.5} + k_4 p_{\mathrm{H_2O}}\right)} \tag{6}$$

Each of the kinetic parameters have an Arrhenius form

$$\ln k_i = A_i + \frac{B_i}{T} \tag{7}$$

where the numerical values have been sourced from Van-Dal and Bouallou.[13] Mignard and Pritchard[14] reasssesed the B_i term for k_1 and k_5 in order to better capture the temperature dependency at varying ratios of CO/CO_2 and was adopted by Van-Dal and Bouallou. The kinetic parameters applied are summarised in Table 1. For simplicity, the formation of DME and higher alcohols have been omitted. Some guidance and inspiration can be found in,[15,16] if this should be included.

Process simulation and flowsheet modelling

The basis for the present work is a replication of the simulation flowsheet for methanol synthesis from syngas published by Luyben.[10] The replication is made in COCO the CAPE-

Table 1: Kinetic parameters as provided in ref.[13] The resulting reaction rate is in kmol/(kg_{cat}s)

i	A_1	B_i
1	-29.87	4,811.2
2	8.147	0
3	-6.452	2,068.4
4	-34.95	14,928.9
5	4.804	-11,797.5
6	17.55	-2,249.8
7	0.1310	-7023.5

OPEN to CAPE-OPEN steady-state simulation environment.[17] For flowsheet modelling COFE v3.7.0.11 (the CAPE-OPEN Flowsheet Environment) is utilised. The replicated flowsheet has been adapted from the Chemsep website and is shown in Figure 1.

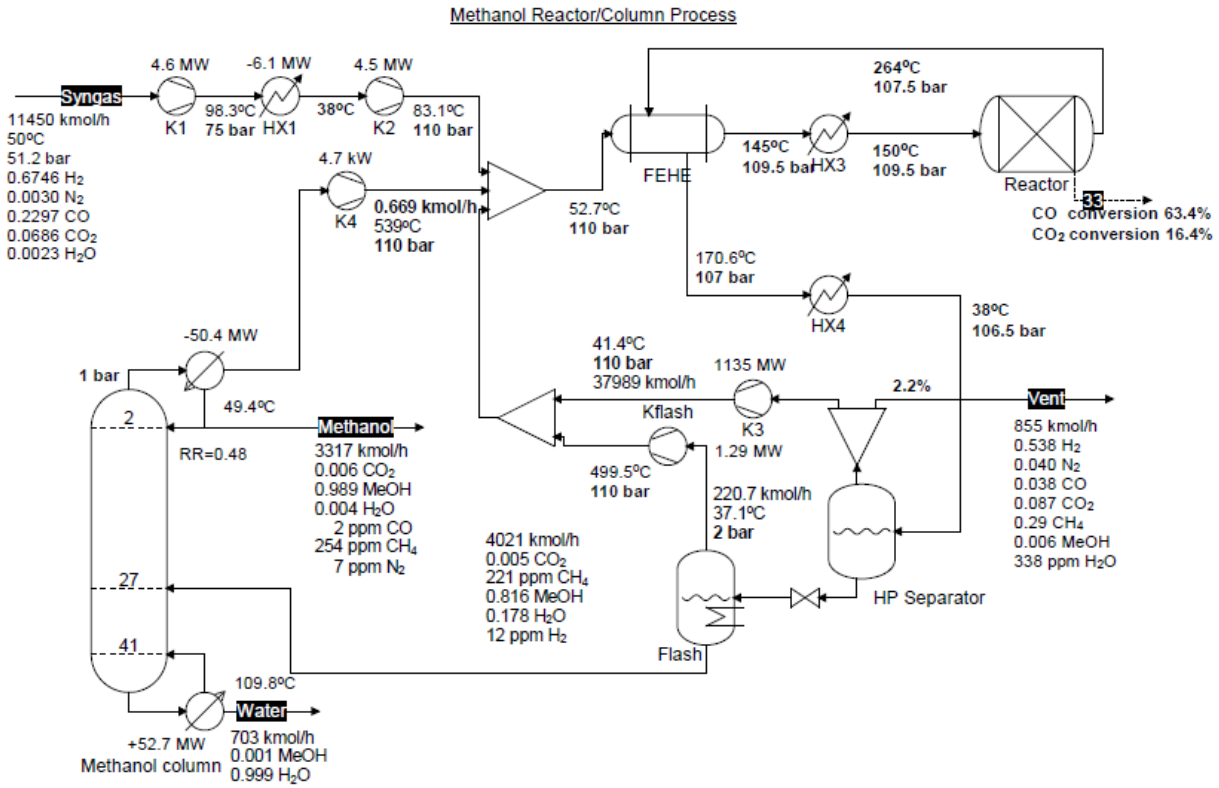

Figure 1: Methanol from syngas process replicated from Luyben[10] in COCO/COFE. The flowsheet is an iteration by the author of the COCO/COFE simulation made by Ross Taylor and Harry Kooijman. The main change is replacing the fixed conversion reactor with a plug-flow reactor with detailed kinetics. The flowsheet is available from the Chemsep website.[18]

COCO/COFE is a steady state sequential chemical flowsheet simulation that is available

free-of-charge. It's design centers around the CAPE-OPEN interface definitions, which are maintained and published by the CAPE-OPEN Laborities Network (CO-LaN[19]) and finds wide use in industry for interoperability of thermodynamic- and unit operation models;[20] it is therefore possible to use any CAPE-OPEN compliant third party thermodynamics server or unit operation model in COCO/COFE; in this research the models that were used were only those that come with COCO itself, as well as those that come with the ChemSep LITE distribution that is installed alongside COCO.

COCO/COFE features a parametric study, but the format in which the study is to be specified does not lend itself for the more complex dependency analysis that is required for techno-economic analysis. Two routes are available to provide a more programmatic approach to studying parametric dependencies: one is via manipulating COFE's input file, which consist of an XML file inside the zip file, and is therefore easily manipulated and analysed using commonly available tools. The other is via COM automation. That route was chosen in this research, in combination with Python's ability to interact with COM objects, using the comtypes package. Additional information about the automation interface for COFE is available via its online help.

For the main flowsheet, the Peng-Robinson equation of state is used[21] for all streams and unit operations except for the Chemsep[18,22] column model which applies the NRTL activity coefficient model (and ideal gas law for the vapour phase) and DECHEMA K-values. For the Peng-Robinson equation of state, default binary interaction parameters are taken from the Chemsep database. The binary parameters for methanol-water have been fitted to experimental data from KDB (Korea Thermophysical Properties Data Bank)[23] using DWSIM[24] as shown with T-xy data at atmospheric pressure in Figure 2. The resulting NRTL paramters are $A_{12} = -245$, $A_{21} = 674$ and $\alpha_{12} = 0.2$ (with 1: Methanol, 2:Water)

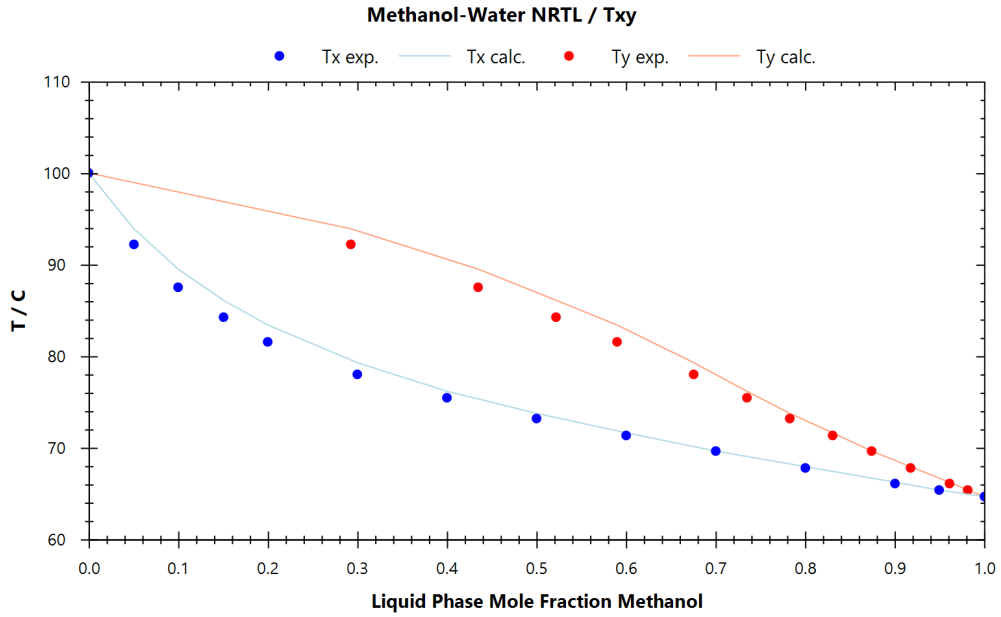

Figure 2: NRTL activity coefficient model for binary methanol and water mixture. Data points sourced from KDB (Korea Thermophysical Properties Data Bank).[23]

CAPEX estimation method

In this study, the capital cost of equipment is estimated using the comprehensive database published by Woods[25] also further elaborated in ref.[26] In Woods,[25] the equipment cost in carbon steel (CS), $C_{Eq,CS}$, is provided in USD at a reference CEPCI index of 1000. This is also referred to as Free On Board (FOB). For most equipment, a base equipment cost is provided for a *reference capacity* with scaling to the actual *capacity* using an equipment-specific sizing exponent, n:

$$C_{Eq,CS} = C_{Eq,CS,ref} \left(\frac{\text{Capacity}}{\text{Capacity}_{\text{ref}}} \right)^{n} \tag{8}$$

The parameters sourced from Woods[25] relevant for the present study are summarized in Table 2 along with their applicable ranges. The cost relations are commented in the following. In case the upper limit of the applicable range is exceeded for e.g. heat exchangers, the required heat transfer area is distributed across several units with the same size, with the individual surface areas summing up to the total required surface area. The heat exchanger

Table 2: Main applied equipment cost relations reported for carbon steel cost in USD and a CEPCI index basis of 1000.

Equipment	$C_{Eq,CS,ref}$ (USD)	Capacity	Capacity$_{ref}$	Unit	n	Range
Vessel/Column	100,000	m	8,000	kg	0.65	$m \in [400, 200000]$
SHE	70,000	A	100	m^2	0.71	$A \in [5, 2300]$
Compressor	1,350,000	P	1,000	kW	0.9	$P \in [2, 7000]$
	10,300,000	P	10,000	kW	0.71	$P \in [7000, 25000]$
Reactor	1,300,000	V	100	m^3	0.4	N/A

costs were estimated based on the overall heat transfer values, U, taken from the original Luyben work.[10]

The applicable power, P, (kW) range in Woods[25] for the cost relations for centrifugal compressors was proposed as $[2, 4000]$ and $[8000, 25000]$. For the purpose of the present study, the two relations were extrapolated up and down, respectively, in order to cover the gap $[4000, 8000]$ by finding the cross-over point between the two relations.

The method described above has been previously implemented for equipment cost estimation by the main author[27] for CAPEX estimation of a biogas upgrading facility including CO_2 compression and heat pumps and for CO_2 compression liquefaction via different open and closed liquefaction schemes.[28] For full plant CAPEX (Total Module Cost), the method described by Woods[25] is also adapted, see also[26] and further desbribed below.

$$C_{\mathrm{BL-L\&M}} = \sum_{k=1}^{n} \left(F_{\mathrm{L\&M,k}} E_{\mathrm{k}} + f_{\mathrm{alloy,k}} E_{\mathrm{k}}\right) \tag{9}$$

$$C_{\mathrm{BL-PM}} = C_{\mathrm{BL-L\&M}} + C_{\mathrm{TFI}} \tag{10}$$

$$C_{\mathrm{BM}} = C_{BL-PM} + C_{\mathrm{offsites}} \tag{11}$$

$$C_{\mathrm{TM}} = C_{\mathrm{BM}} + C_{\mathrm{CF}} + C_{\mathrm{CF}} + C_{\mathrm{C1}} + C_{\mathrm{C2}} \tag{12}$$

where E_k is the Free Onboard equipment cost of equipment k in carbon steel, f_{alloy} is the alloy factor for equipment, k, $F_{L\&M,k}$ is the labour and materials cost for installation of equipment k and includes all ancillary materials such as piping, structure, electrical, foundations etc. $C_{BL-L\&M}$ is the ISBL cost of installed equipment, C_{TFI} is the cost for tax, freight and insurrance, C_{BL-PM} is the ISBL physical module cost. $C_{offsites}$ is the cost of offsites + indirects for home office and field expenses incl. engineering and project management. C_{BM} is the bare module cost, adding contractors' fee C_{CF}, contingencies for delays C_{C1} and contingencies for scope changes C_{C2}, the total module cost is found. Provided that the OSBL cost for cooling and heating will be accounted for in OPEX, the simplification of equalling the total module cost with the total plant cost is made. The applied factors are summarised in Table 3.

Table 3: Applied factors for the Wood's cost model and recommended ranges.[25] An additional allowance of 25% is added for OSBL cost other than cooling and heating.

Cost factor	Range (%)	of	Woods (%)
C_{TFI}	20	$E_k f_{\mathrm{alloy,k}}$	15-25
C_{offsites}	27.5	$C_{BL-L\&M}$	10-45
C_{CF}	4	C_{BM}	3-5
C_{C1}	12.5	C_{BM}	10-15
C_{C2}	20	C_{BM}	10-30

OPEX and levelised cost calculation

For case comparison, the total CAPEX is used as one indicator. However, the total CAPEX does not consider annualised costs. Annual costs include several other factors such as fixed operations and maintenance costs (FOPEX), variable operations and maintenance costs (VOPEX) in addition to the annualised CAPEX. A Levelised Cost, for the purpose of this study referred to as Levelised Cost of Methanol, LCOM, factors this in. Especially the variable cost of electricity required for compression can be an important factor. For example, a high CAPEX case with low power requirements may provide a lower LCOM than a low CAPEX case with high power requirements (depending on the difference in CAPEX and the

cost of electricity). In this study, the simplified definition of levelised cost in analogy with NREL's Levelised Cost of Energy (LCOE)[29] which assumes overnight capital cost and O&M costs being invariant over the years[1] is applied. The LCOM is hence given as:

$$\mathrm{LCOM} = \frac{\mathrm{CRF} \cdot \mathrm{C_{TM}} + \mathrm{O\&M_{fixed}} + \mathrm{O\&M_{variable}}}{\int_{t=0}^{1year} \dot{m}} \tag{13}$$

In Equation 13, CRF is the capital recovery factor; C_{TM} is the overnight capital cost as calculated from Equation 12; $O\&M_{fixed}$ is the yearly fixed Operations and Maintenance cost invariant of the plant load/capacity and $O\&M_{variable}$ is the yearly Operations and Maintenance cost that scales with plant load cf. 4. The denominator in Equation 13 is the yearly amount of produced methanol, which we set as the nominal mass flow (kg/s) integrated over the year, assuming 8,000 hours at the design rate. The variable O&M costs will, for simplicity, be set at the cost of reactants, cost of electricity to power compressor, cost of cooling and cost of heating, respectively.

The capital recovery factor is defined as:

$$\mathrm{CRF} = \frac{i(1+i)^n}{(1+i)^n - 1}, \tag{14}$$

where i is the interest rate and n is the number of annuities over the project lifetime. In this study, the interest rate is set to 8% ($i = 0.08$) and the project lifetime is set to 20 years ($n = 20$). The fixed O&M cost is often expressed as a fraction of the overnight costs. Typical values quoted are in the range of 2-6%, depending on the source of information and the process plant type.[30–32] For the sake of simplicity, other fixed costs such as insurance, property taxes, rent of land etc., have not been specifically accounted for, however in the present study O&M costs are fixed to 3% of the total CAPEX.

[1] `https://www.nrel.gov/analysis/tech-lcoe-documentation.html`

Table 4: Variable OPEX input to techno-economic analysis. The levelised cost of hydrogen is from European Hydrogen Observatory cost calculator, assuming offshore wind, alkaline electrolyzers in Denmark. It should be noted that this value is only approx. half of that stated by TNO.[33]

	Unit	Value	Description
Electricity	USD/MWh	70	
Utility cooling	USD/MWh	1.36	From[34]
LP Steam for heating	USD/MWh	28	From[10]
Grey hydrogen	USD/kg	2	From[35]
Green hydrogen	USD/kg	6.82	From[36]
Captured CO_2	USD/t	70	From[37]

Surrogate modelling and optimisation

A surrogate model of the process simulation model is built by running the process simulation model for each record in a sampling plan. For each sample, the process parameters are varied, and a combination of the sampling plan with the recorded simulation output, serves as input for the surrogate model training. An automated process of running all the computer experiments defined by the sampling plan is made combining the process simulator with Python (programming language) via COM (Microsoft Component Object Model) . A black-box wrapper is made in Python exposing the process simulation as an object which can be called like a regular function, taking the defined factors/independent variables as input, and returning the desired defined output(s), when the simulation has converged. A similar black-box approach has been used by others[38–42] using either VBA, python or Matlab/Octave as programming layer. For each sample in the sampling plan, a corresponding simulation is made and the results recorded.

In the present study, two approaches are taken, the first is using DACE (Design and Analyis of Computer Experiments) via a Box-Behnken 3-factor design and applying Response Surface Methodology (RSM). An exhaustive presentation of the methods of DoE and RSM will not be given here. Instead the reader is referred to relevant textbooks and literature.[43,44]

The general second order response surface model can be expressed as

$$y = \beta_0 + \sum_{i=1}^{k} \beta_i x_i + \sum_{i=1}^{k} \beta_{ii} x_i^2 + \sum_{i=1}^{k} \beta_{ij} x_i x_j \tag{15}$$

By linear regression analysis,[45] the coefficients (β) can be estimated. It often turns out that some of the effects (usually second-order terms) are statistically insignificant and can be excluded from the model by either e.g. step-wise linear regression or a criterion based strategy.[45] The response surface model is optimised using the SLSQP algorithm[46] in order to find process parameters and operating conditions for optimial grey methanol production for comparison with previous pubulished data.[10]

The other approach taken in the current study is using a Kriging surogate model for optimisation. The sampling is generated as an optimized Latin-Hypercube design[47,48] by the pyKriging package.[49] It is suggested that for up to 10 variables, a sampling size of 10-15 times the number of variables should suffice.[50,51] In the present study, a sampling size 20 times the number of variables has been applied, which has been used with good experience previously by the author.[38,41]

The sampling plan and recorded simulation model output is used to train a Kriging model[52–54] using the pyKriging package.[49,55,56] See also[38,40,57,58] for other examples and more information about Kriging in chemical engineering applications. Surrogate models are built for various simulation / techno-economic output: LCOM, CAPEX, OPEX, Power requirement, Methanol production. The validated surrogate models are used to estimate process parameters and operating conditions for optimal green methanol production.

Results and discussion

Kinetic model validation

The applied kinetic model as implemented in COCO/COFE is compared to the same kinetic model as implemented by Van-Dal and Bouallou as well as the originally developed model by Vanden Bussche & Froment in Figure 3. The results shown are for a plug-flow micro-reactor simulation. As seen, the simulations in COCO/COFE perfectly match the Van-Dal and Bouallou implementation. The difference to the original model of Vanden Bussche & Froment in the first part of the catalyst bed has been rationalised[13] in terms of the adjustment of activation energies made by Mignard & Pritchard.[14]

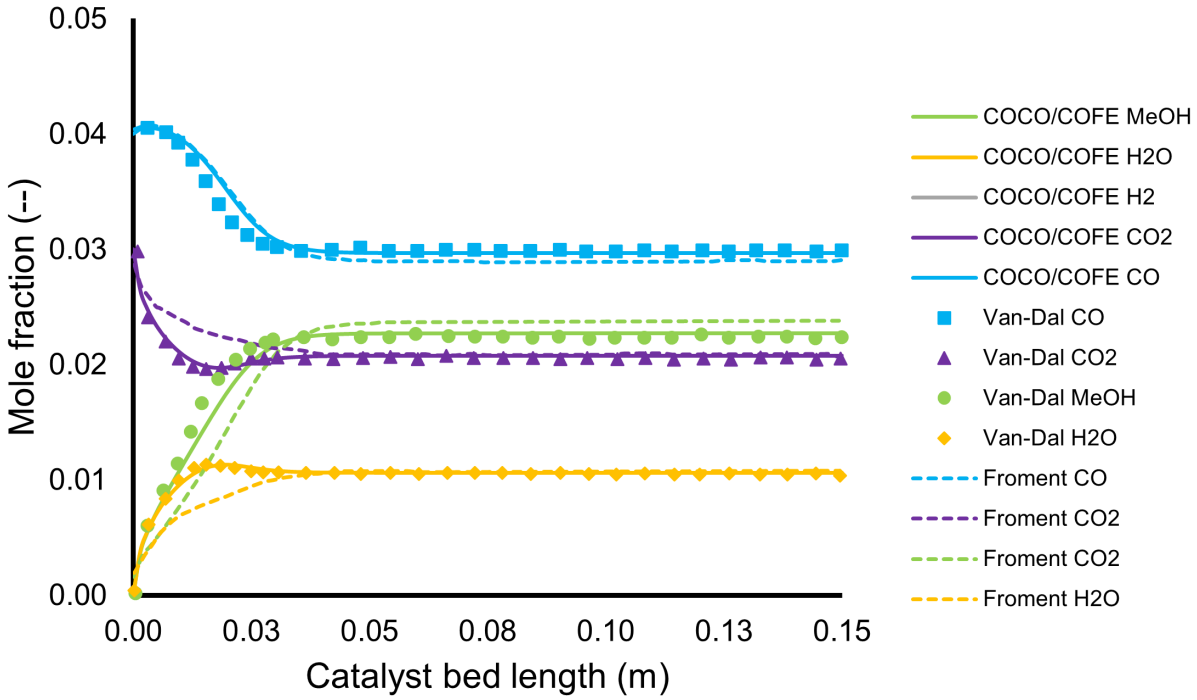

Figure 3: Mole fraction as a function of catalyst bed as simulated with COCO/COFE compared to the simulations of Van-Dal & Bouallou[13] and Vanden Bussche & Froment.[12] $P = 50$ bar, $T = 220°$C, $\dot{m} = 2.8 \cdot 10^{-5}$ kg/s, Reactor diameter $D = 0.016$ m, $y_{CO} = 0.04$, $y_{H_2} = 0.82$, $y_{CO_2} = 0.03$, $y_{inert} = 0.11$, $\rho_{cat} = 1775$ kg/m^3, $\phi = 0.5$, Pellet diameter $d_p = 0.0005$ m.

To further test and build confidence in the applied kinetic model, the experimental data

for conversion of CO/CO_2 to methanol published by Klier *et al.*[59] is simulated. The results are shown in Figure 4. As seen, the implemented kinetic model predicts a trend which is in good agreement with the experimental data. The optimum in carbon conversion to methanol occurs at 2% CO_2 / 29% CO as in the experimental data, with a conversion going towards zero at CO-free feed gas composition. At higher CO_2 concentrations ($> 2\%$) i.e. lower CO concentrations, the carbon conversion also decreases as seen experimentally.

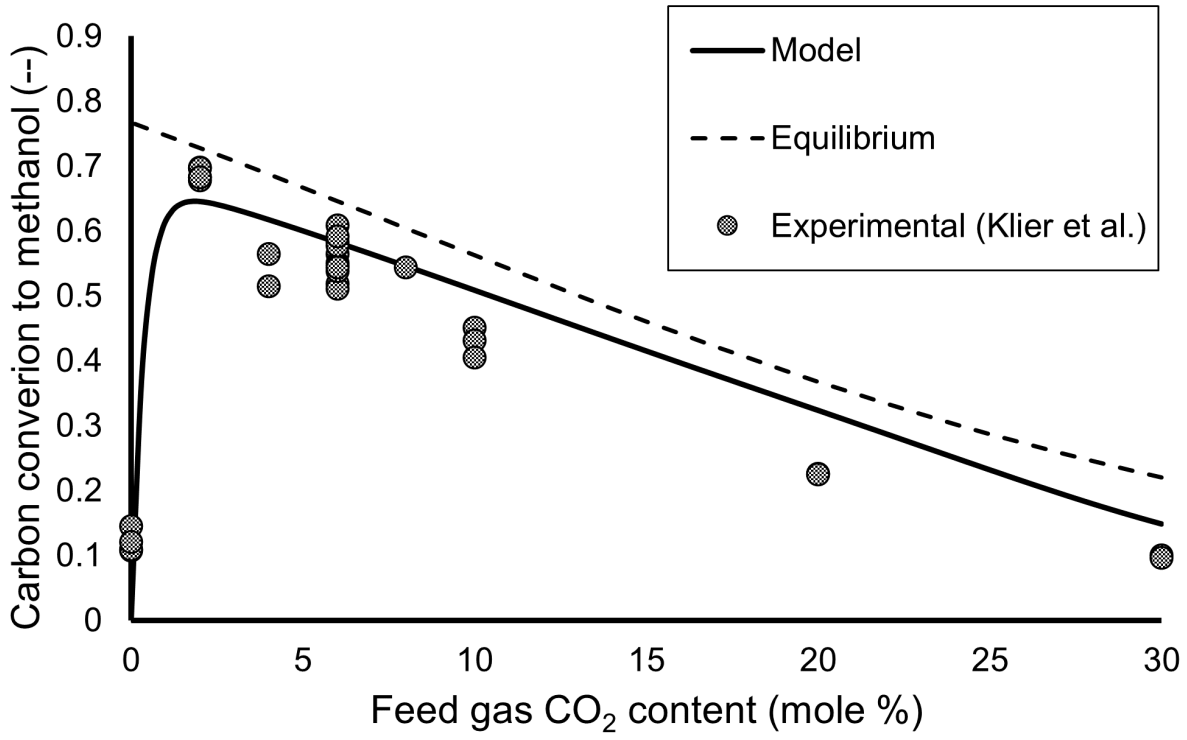

Figure 4: Carbon conversion to Methanol as a function of CO_2 content in the feed at 75 bar and isothermal conditions at 250°C. The CO content is $30 - x$, with x equal to the CO_2 content. The molar fraction of hydrogen is kept constant at 70%. Experimental points have been extracted from the work of Klier *et al.*[59]

Simulation model validation - Luyben revisited

Key figures have been extracted from the basis simulation file in COCO/COFE and compared to the results from Luyben.[10] The results are summarised in Table 5 and Table 6.

Table 5 compares energy streams for compressors and heat exchangers (FEHE included

Table 5: Comparison between energy streams in the applied COFE/COCO basis simulation model and the data from.[10]

	Unit	COCO/COFE	Luyben	Diff (%)
K1	MW	4.62	4.5	2.8
K2	MW	4.47	4.48	-0.2
K3	MW	1.14	1.175	-3.4
Kflash	MW	1.29	1.341	-4.0
K4	kW	4.76	4.9	-2.9
HX1	MW	6.13	5.71	7.3
FEHE	MW	44.5	44.3	0.4
Reactor	MW	29.5	28.3	4.3
HX3	MW	2.42	2.99	-19.0
HX4	MW	99.5	102	-2.4
Reboiler	MW	52.7	54.82	-3.9
Condenser	MW	50.4	47.34	6.5

although this is a cross-heat exchanger for heat recovery). For all compressors, the energy requirement deviates less than 4%. The heat exchangers in feed gas compression and the synthesis loop, show deviations at a comparable level with some exceptions. HX1 after the first stage feed compression deviates more, which is also linked to a higher compression power requirement. The one exchanger with the highest relative difference is HX3 upstream the reactor, but the absolute difference is only moderate.

Table 6 shows flow and composition of the methanol product from the distillation column as well as the overhead vapour. The total amount of produced methanol matches very closely. Some impurities such as CO and N_2 in particular differ significantly, yet the final purity is identical. The overhead vapour matches very well in terms of total flow. Some differences are observed for the split between methanol and carbon dioxide and hydrogen and methane content. As seen from Table 5 the reboiler and condenser duty also shows some minor discrepancies. It is most likely due to different choices of VLE models. Luyben[10] applied the van Laar activity coefficient model, whereas the present study employs the NRTL model.

The per pass conversions are compared in Table 7 and are quite similar, although an exact comparison is difficult due to less significant digits in the Luyben paper. The total molar flow recycled is 38,210 kmol/h compared to 39,863 kmol/h as simulated by Luyben. The main

Table 6: Comparison of the overhead vapour stream and the methanol product stream leaving the distillation column between the applied COFE/COCO simulation model and the data from.[10]

		Methanol product	
Parameter	Unit	COCO/COFE	Luyben
Total flow	kmol/h	3317	3311
MeOH	mole fraction	0.989	0.989
CO_2	mole fraction	0.006	0.009
H_2O	mole fraction	0.004	0.001
CO	ppm	2	896
CH_4	ppm	255	198
N_2	ppm	7	727
		Overhead vapour	
Parameter	Unit	COCO/COFE	Luyben
Total flow	kmol/h	0.669	0.669
MeOH	mole fraction	0.512	0.545
CO_2	mole fraction	0.390	0.421
H_2	mole fraction	0.025	0.018
CH_4	mole fraction	0.067	0.014

difference is probably the slight difference in the applied kinetic model and parameters, i.e. inclusion of the modifications by Mignard & Pritchard.[14] Using the total molar flow entering the reactor of 49,660 kmol/h and 51,313 kmol/h for COCO/COFE and Aspen Plus (Luyben), the calculated Gas Hourly Space Velocity (GHSV) is 10,689 h^{-1} vs 11,250 h^{-1}. All in all, the COCO/COFE model displays higher reaction rate towards methanol / higher hydrogen conversion, likely attributed to the difference in the applied kinetic parameters. A side effect is also an increased heat extraction from the reactor, a sligh reduction in recompression power and a slightly reduced cooling duty required upstream the HP separator. Still, the results are indeed comparable and much alike despite differences in simulation tools, difference in thermodynamic and kinetic models and parameters.

Table 7: Comparison of per pass conversion between the applied COFE/COCO basis simulation model and the data from ref.[10]

	Unit	COCO/COFE	Luyben	Diff.
H_2	%	25.8	25	0.8
CO_2	%	16.4	17	-0.6
CO	%	63.4	64	-0.6

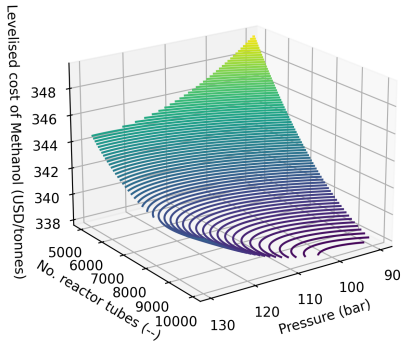

Minimum purge/vent rate 1.5%

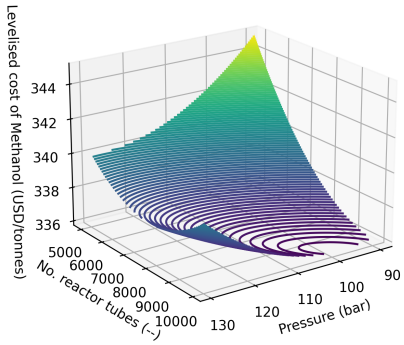

Optimal purge/vent rate 2.2%

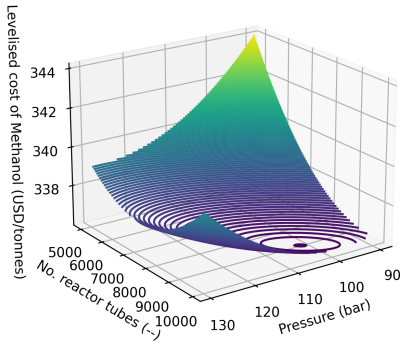

Maximum purge/vent rate 2.5%

Figure 5: Response surface for minimum, optimal and maximum applied vent/purge rate.

For further comparison with the results of Luyben, an optimisation study is performed

using the simulation in Figure 1 using a Box-Behnken experimental design for generating model outputs which are used to train a response surface model as surrogate of the actual process simulation e.g. as shown in.[60] The following independent variables / factors are varied: compression/reaction pressure (pressure after K2 compressor), reactor size (via the number of reactor tubes), and the purge/vent percentage. Luyben also investigated the flash pressure in the low pressure flash separator, however, for simplicity this is omitted. For each dependent variable / response, a multiple regression model is built which includes all first order terms, second order terms and linear interaction terms, with backward elimination of insignificant second order and interaction terms. The simulation model in Figure 1 is modified slightly by removing HX3 and setting the outlet of FEHE towards the methanol reactor to 150°C.

Selected response surfaces are visualised in Figure 5. The optimal settings are found using constrained optimisation using Sequential Least Squares Programming (SLSQP),[46] and minimum LCOM occurs with a purge/vent rate of 2.26%, a pressure of 99 bar and 9680 reactor tubes. As seen from Figure 5, a higher purge rate shifts the optimum towards fewer tubes i.e. less catalyst volume, due to a lower recycle rate and accumulation of inerts and vice versa for a lower purge rate. The optimal purge rate is very close to the value of 2.2% found by Luyben using a one-factor-at-a-time (OFAT) approach. Luyben found very little difference between 9,000 and 10,000 tubes, with a slightly better economy at the high end. Luyben selected 110 bar based on an analysis of return of investment (ROI), whereas a lower optimal pressure is suggested in this study. Despite the different objectives chosen (levelised cost, vs income/ROI), the conclusions are very similar. The reason for a slightly lower pressure found to be optimal in the present study may also, at least partially, be due to a slightly better conversion due to the differences in kinetic parameters applied.

Heat integration

FEHE/Reactor heat recovery (option 1) This scheme involves increased heat recovery in FEHE, thereby increasing reactor feed gas temperature, making more of the reaction heat available from the reactor steam generation to heat the distillation column reboiler.

Direct reboiler waste heat utilisation (option 2) This scheme uses the available heat down to 122.5 °C upstream HX4 as direct heat source for the distillation column reboiler leaving a comfortable pinch of 12°C. The remaining heat required for the reboiler is provided by steam from the reactor.

Distillation column pre-heat (option 3) This scheme uses heat upstream HX4 to pre-heat the feed to the distillation column and the remaining heat required for the reboiler is provided by steam from the reactor.

It has already been proven that methanol synthesis (even via direct hydrogenation) can be made thermally self-sustained.[61] Although the process studied so far does not have full heat integration (except FEHE exchanger), the surplus heat generated in the reactor (29.5 MW), combined with the methanol/syngas cooler/condenser HX4 (99.5 MW) as seen from Table 5, exceeds the heat input required for the distillation process reboiler (52.7 MW). However, not all the excess heat from HX4 is available at the required temperature level. Further, different heat integration schemes may be more optimal than others. In the following, different heat integration schemes are investigated.

The flow diagrams of the different heat integration schemes are shown in Figure 6. The key results for the different heat integration options are summarised in Table 8. Comparison is made against the base case which is the Luyben model with the slight modification of HX3 being excluded. As seen from Table 8, all heat integration options result in reduced OPEX and levelised cost of methanol despite higher CAPEX (not correcting CAPEX for reduced balance of plant due to reduced cooling utility requirement, only OPEX is corrected). Of the

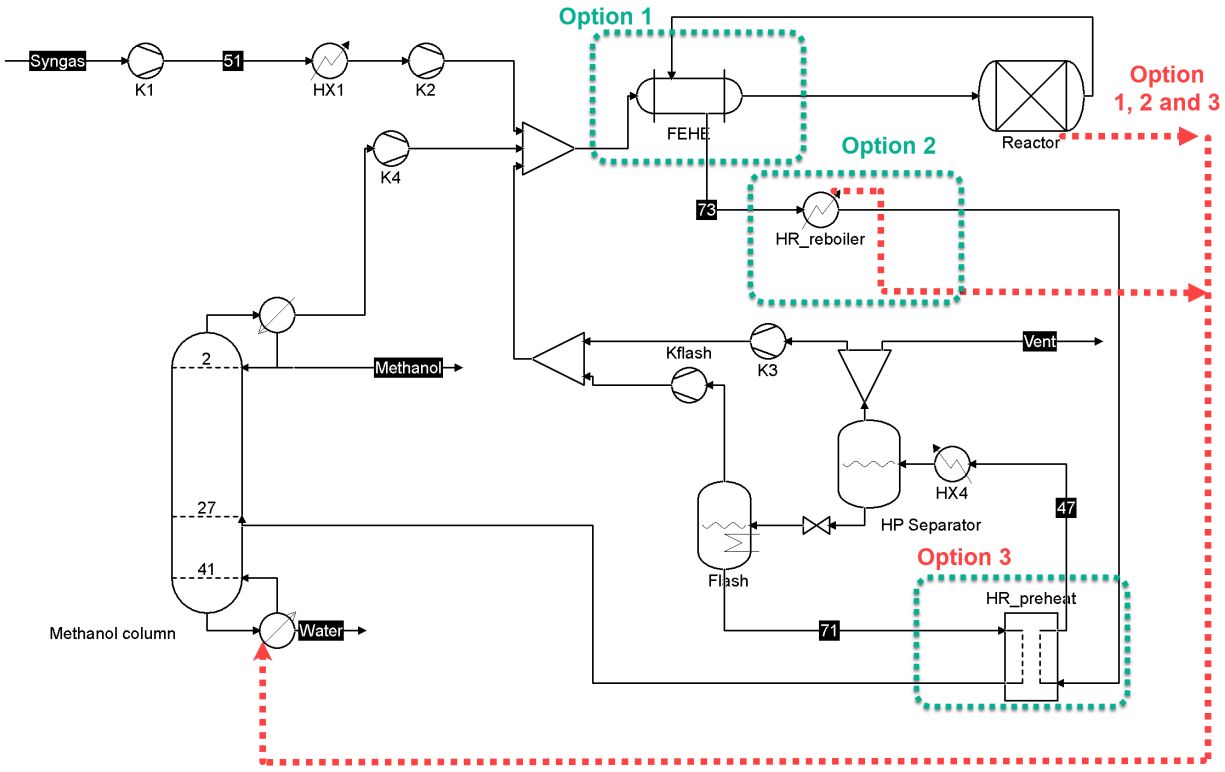

Figure 6: Methanol from syngas process with various heat integration options. Red dashed lines symobolise heat recovery streams used in the distillation column reboiler. In all cases is the steam generated in the methanol synthesis reactor used as heat source for the reboiler.

three investigated heat integration options, the third option which recovers heat upstream HX4 by cross exchange with cold methanol/water from the Flash separator (thereby partially flashing the feed to the distillation column) appear the best, yet only marginally. The best improvement in LCOM is 5.2 USD/tMeOH or 1.5%.

Table 8: Different heat integration options and the correpsponding CAPEX, OPEX and levelised cost. Q_{heat} is the net external heating requirement.

Case	CAPEX (10^6 USD)	OPEX (10^6 USD/y)	LCOM (USD/t)	Q_{heat} (MW)
Base	176.1	265.4	337.3	23.2
1	186.3	260.2	332.4	0
2	190.6	260.4	333.1	0
3	184.4	260.2	332.1	0

Green methanol TEA and optimisation

For the base case, a flowsheet and heat integration setup is made combining option 2 and 3 as per Figure 6. The feed to the process is a 75/25 mixture of hydrogen and carbon dioxide. A small quantity of nitrogen is included as a proxy for inerts mainly from the carbon capture process. The process is made self-sufficient in heating for the methanol distillation column with a slight surplus in heat from the methanol reactor unutilised. The integration of the heat from the reactor into a steam-driven pre-heater upstream the reactor has already been demonstrated by[61] but for simplicity this is not implemented.

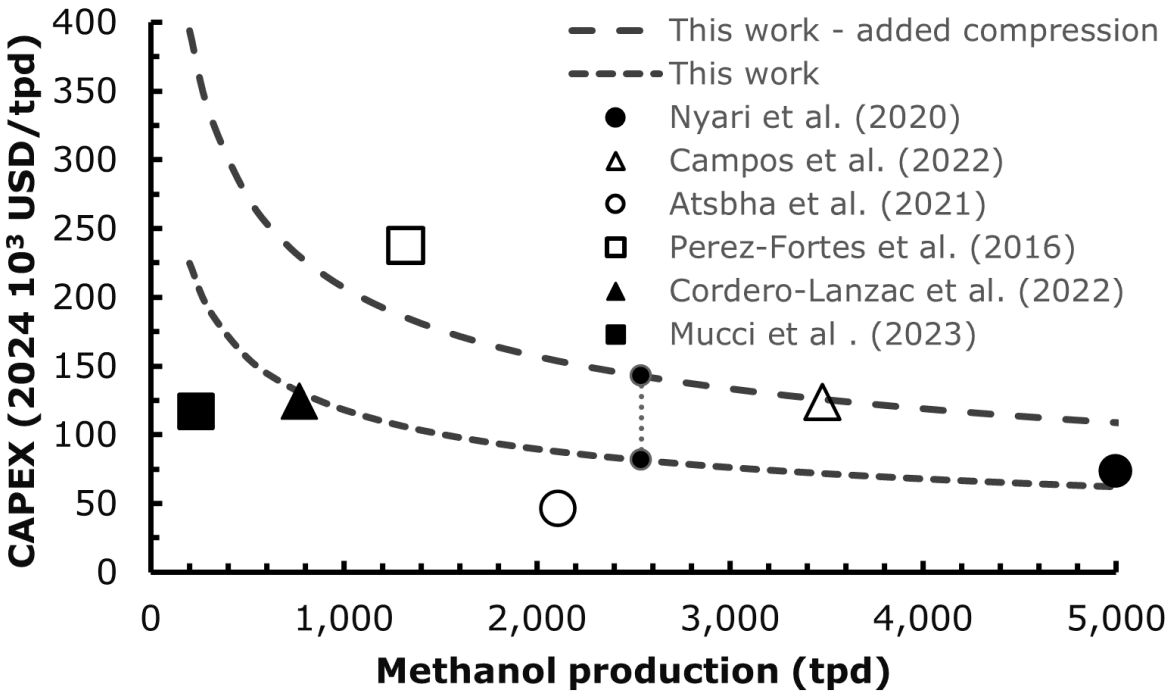

Figure 7: Specific CAPEX of methanol production via direct hydrogenation of CO_2 and H_2 compared to literature values. Literature data has been cleaned from added working capital. All data has been corrected to the same cost index. Data has been generated using a reactor feed pressure of 100 bar, a boiling water reactor temperature of 260° C, a catalyst bed volume of 150 m^3, and a purge rate of 1%.

The total CAPEX estimated for the base case is compared to other literature studies[7,8,62–65] in Figure 7. A single point CAPEX estimate for the present study at 2,540 tonnes MeOH/day is extrapolated via a 6/10th rule. Most of the referenced studies include com-

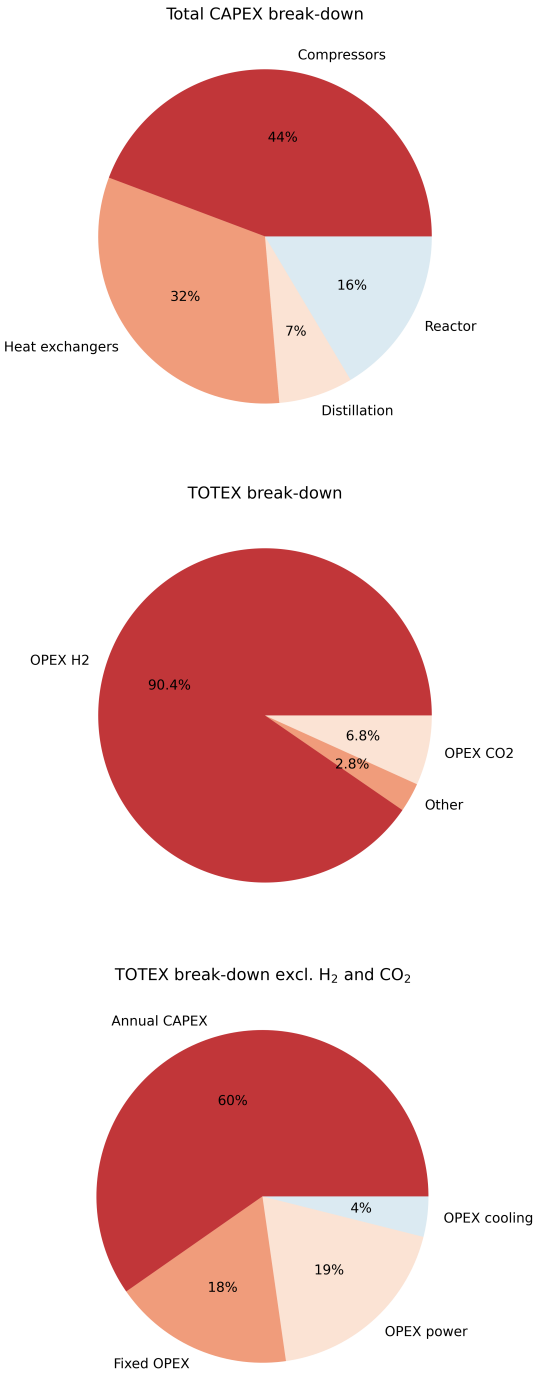

Figure 8: Techno-economic analysis of green methanol production via direct hydrogenation of captured CO_2 and H_2 produced from electrolysis. Data has been generated using a reactor feed pressure of 100 bar, a boiling water reactor temperature of 260° C, a catalyst bed volume of 150 m^3, and a purge rate of 1%. The total CAPEX is 206.6 million USD and the resulting LCOM is 1,472 USD/tonne MeOH.

pression of CO_2 from atmospheric pressure and hydrogen compressed from approx. 30 bar. In order to make a fair comparison, an adjusted CAPEX is made including the same level of compression (the base case compresses H_2/CO_2 from 51.2 bar). As seen from the results, there is a wide spread in the estimated CAPEX. The results of the present study are in close agreement with the results of Campos *et al.*[8] The results of Nyari *et al.*[64] are also comparable to the estimates of the present study, considering that hydrogen compression is from 50 bar and CO_2 compression is from 2 bar. Thus, it would be expected to fall within the two cost curves, as is also observed. The work of Perez-Fortes *et al.*[62] is higher than the comparable cost curve, but this may partially be explained by hydrogen compression being from 25 bar instead of 30 bar. On the other hand, the CAPEX from Atsbha *et al.*[7] and Mucci *et al.*[65] seems to be under-estimated, also to some extent the work of Cordero-Lanzac *et al.*[63] In general the CAPEX modelling provided in the present study seems to be of sufficient quality for techno-economic analysis of green methanol production.

The techno-economic summary of the proposed process base case using somewhat arbitrary, yet meaningful process parameters, is shown in Figure 8. The distribution of CAPEX for the main components is similar to that shown by Pérez-Fortes *et al.*[62] They estimated compressors to be the biggest share of purchased equipment cost with 45% of the total, and heat exchangers to be the next biggest contributor with 40.6%. However, a discrepancy is the estimated cost of distillation and reactor, which was estimated to be only 1% and 1.5% by Pérez-Fortes *et al.*,[62] much lower than in the present study. Cordero-Lanzac *et al.*[63] found compressors to be, by far, the biggest contributor to purchased equipment costs, which is amplified due to compression from 1 bar compared to the 51.2 bar assumed in the current study. Vaquerizo and Kiss[61] found similar trends with the following order of CAPEX contributions: Compressors, Heat exchangers, Reactor, Distillation. Very similar to the current study, also acknowledging compression from a lower pressure in the cited study.

The total annual expenditure (TOTEX) is heavily determined by the cost of hydrogen and carbon dioxide supply with hydrogen being the dominant factor. Almost 97% of the

Table 9: Validation statistics for the surrogate models.

Response	R^2	R^2_{adjust}	RMSE	RMSE(normalised)
Levelised cost	0.9989	0.9989	0.8155	0.0005
CAPEX	0.9944	0.9942	1725689	0.0083
Power	0.9989	0.9988	0.0689	0.0059
OPEX	0.9974	0.9973	92370	7.5405e-05
MeOH production	0.9999	0.9999	108.82	0.0001

TOTEX is due to reactant supply. The other elements being annualised CAPEX, fixed and variable OPEX (cooling and electricity). Of the other contributors, annualised CAPEX is the biggest contributor, followed by electricity cost, fixed OPEX and cost of cooling being the smallest fraction of TOTEX.

The base case is further explored and used in LHS and surrogate model training via the automation wrapper. In order to simplify the convergence of the simulation model when generating the training set for the surrogate model, a fixed duty of the *HR_preheat* cross heat exchanger (as seen in Figure 6) is assumed. However, this leads to the heat balance for the reboiler not being maintained in all simulations. This simplification is justified by the fact that the cost of heat integration and the effect on CAPEX, OPEX and LCOM is fairly constant as demonstrated in Table 8. The following independent variable are considered: reactor loop feed pressure (downstream K2), reactor catalyst volume, temperature on the boiling water side of the reactor tubes, and the purge rate. The following lower/upper bounds are considered: 75–125 bar, 100-239 m^3, 240–270°C and 0.5-2%, respectively.

The surrogate model performance is compared to direct simulation results for a test data set with 40 points not used in the training of the surrogate model. Graphical comparison is made in Figure 9 and validation statistics are included in Table 9. As seen from the results, the surrogate models for LCOM, CAPEX, Power, OPEX, and methanol production shows good performance and fidelity for being used as a replacement of the full simulation model in optimisation.

Using the surrogate model developed for LCOM, optimisations are run for finding the settings providing the lowest LCOM within the bounds of the independent variables. Both

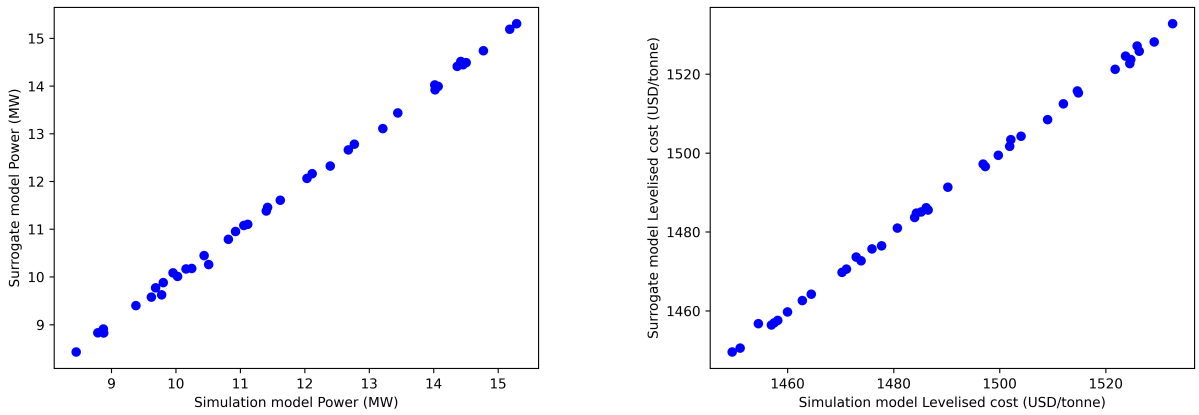

(A) (B)

Figure 9: Surrogate model (Kriging) result versus direct simulation (black-box) result for (A) total power requirement for compression and (B) Levelised cost of methanol.

local (SLSQP, Powell and Nelder-Mead) and global optimisers (Differential Evolution, Simplicial Homology Global Optimization and DIviding RECTangles) are probed, all available in the `scipy` module.[66] The results of the optimisation is summarised in Table 10. As seen, the optimisers finding the lowest minimum are SLSQP, Differential Evolution and SHGO. The results show that the SLSQP algorithm is capable of finding basically the same optimum as the SHGO algotrithm. This could indicate that the optimisation problem is convex, and fairly well behaved, although not proved. The minimum LCOM is found with the purge at the lower bound, which can be justified from the fact that less valuable reactants are lost (especially hydrogen is expensive) in the purge stream thereby reducing methanol production/efficiency. The pressure is somewhat lower than found for the Luyben process described previously (100–110 bar), and also the temperature on the boiling water side of the reactor is a bit lower (compared to 267°C). The catalyst volume is optimal in the higher end, but not at the upper bound. Apparently, the incremental benefit of increasing the catalyst bed volume further is not justified due to increased CAPEX of the reactor. Compared to the base case which has an LCOM of 1,472 USD/tonne MeOH, the optimised LCOM is 1,447 USD/tonne MeOH cf. Figure 8, a reduction of 1.7% despite an overwhelming dominance by the price of hydrogen. The CAPEX is reduced from 206.6 million USD to 179.7 million

USD, a significant reduction of 13%. This clearly display the benefit of performing such multi-parameter optimisation.

Table 10: Optimisation results for Levelised Cost of Methanol (LCOM) using Kriging surrogate models and various optimisation methods.

LCOM (USD/tonne)	Pressure (bar)	Temperature (°C)	Purge (–)	Catalyst volume (m^3)	Optimizer	Type
1,446.7	78.4	253.8	0.005	196.9	SLSQP	local
1,447.9	92.4	258.7	0.005	203.6	Powell	local
1,447.9	82.8	253.9	0.005	239.0	Nelder-Mead	local
1,446.7	77.6	253.8	0.005	186.9	DE	global
1,446.7	78.5	253.8	0.005	196.8	SHGO	global
1,446.8	78.6	253.9	0.005	197.5	DIRECT	global

Table 11: Optimisation results using the SHGO algorithm for all model responses and corresponding independent variables (factors). The response being optimised is highlighted.

Responses					Factors			
LCOM (USD/t)	CAPEX (10^6 USD)	Power (MW)	OPEX (10^6 USD/y)	MeOH (t/d)	Pressure (bar)	Temperature (°C)	Purge (–)	Cat. Vol. (m^3)
1,446.7	179.7	8.73	1,222.7	2,570.6	78.5	254	0.005	196.8
1,505.9	**171.7**	8.11	1,221.8	2,467.4	76.2	252	0.017	216.2
1,510.3	172.1	**7.90**	1,221.8	2,458.6	75.0	253	0.018	227.8
1,521.0	169.8	8.27	**1,221.7**	2,438.9	75.0	251	0.020	187.2
1,452.9	232.0	13.59	1,226.6	**2,582.6**	116.8	265	0.005	207.5

Optimisations are performed for all responses with the corresponding trained surrogate models i.e. CAPEX, OPEX, Power and methanol production in addition to the levelised cost. The results are summarised in Table 11. As seen from the results, most optimisation targets favor operating pressure in the lower end of the investigated range, except when methanol production is being maximised. Also in terms of optimal temperature, the maximum methanol production appears to favor a temperature slightly higher than for the other optimisation targets. The purge rate is at its minumum value for both minimal LCOM and maximum methanol production. In the calculation of LCOM, the methanol production is a strong factor (denominator), hence the similarity. For the other targets, CAPEX, Power and OPEX, the purge rate is high which leads to lower compression power and therefore

also to reduced CAPEX (smaller compressors installed), and also the derived effect of both lower fixed OPEX (due to lower CAPEX) as well as lower variable OPEX due to lower power consumption. The minimum OPEX and Power is obtained when the operating pressure is the lowest, which is due to lower CAPEX for equipment at lower design pressure. The lowest power case has the highest reactor/catalyst bed volume, since this leads to lower pressure drop for a fixed reactor length, and higher conversion and hence lower compression for the reduced recycle. Compared to the case of methanol production from syngas, optimality is generally obtained at lower operating pressure, higher reactor bed volume, slightly lower reactor temperature and significantly reduced purge rate.

It is interesting to note the obvious competing forces between different optimisation targets and how two different optimisation targets can lead to widely different designs. Clear examples are the duality between lowest LCOM and highest methanol production in terms of optimal operating pressure and also seen in the slightly different resulting CAPEX and power requirement. Also the duality between the minimum power case and the minimum LCOM case in terms of the widely different applied purge rates is noted. On the other hand, it is noted that the lowest CAPEX, Power and OPEX, are quite similar, since the power requirement has a strong first order effect on both CAPEX and OPEX. Another interesting observation is the fact that the minimum LCOM optimisation also carries penultimate optima from the other cases e.g. the power, OPEX and CAPEX for the LCOM optimal case is not the lowest, but significantly lower than the worst case (MeOH production maximum), the methanol production is not the highest, but still significantly higher than the optimal CAPEX, OPEX and power cases, not far from the MeOH optimal case. Thus, the minimum LCOM is an apparent result of pareto optimality in OPEX, CAPEX and MeOH production.

The pareto optimimality is further visualised in Figure 10 where multi-objective optimisation has been performed for the three responses CAPEX, power requirement and methanol production using the NSGA-II algorithm[67] provided by the `platypus` library.[68] As seen, the minimum LCOM is close to a pareto optimial solution, which can be seem from the pareto

frontier. Methanol production cannot be improved further without substantial increase in power requirement and CAPEX.

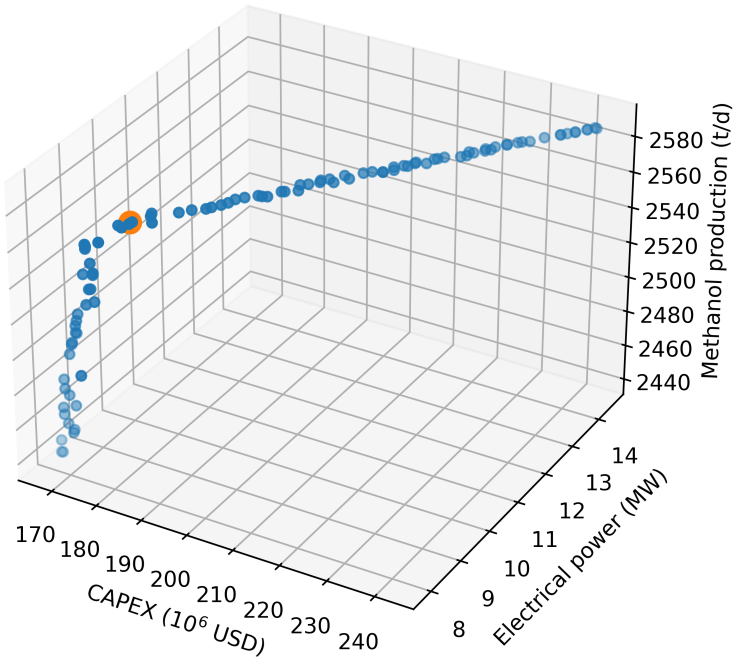

Figure 10: Pareto frontier for multi-objective optimisation of CAPEX, power requirement and methanol production. Blue points are non-dominated solutions to the multi-objective optimisation and the red point is the solution representing optimal LCOM as found from the single objective optimisation using the SHGO algorithm.

Conclusion

In this paper, the public domain process simulation software COFE/COCO has been applied in combination with automation via python to perform techno-economic optimisation of both grey and green methanol. Starting with a previously published process flowsheet based on Aspen Plus adapted to COFE/COCO and thoroughly benchmarked and validated both in terms of the kinetic model applied as well as the overall heat and mass balance, a techno-economic optimisation was performed with response surface methodology applying a Box-Behnken design for three independent parameters: reactor loop feed pressure, num-

ber of reactor tubes (with catalyst) and the purge rate. The optimisation performed on the response surface model, revealed minimum levelised cost of grey methanol at a purge rate of 2.26%, a reactor feed pressure of 99 bar, and 9680 tubes at fixed length and diameter. The results are in good agreement with the conclusions drawn by Luyben,[10] the author of the original model. Different heat integration options were investigated and it was generally found that heat integration with the intent to provide all heat required for the reboiler in the distillation/purification is beneficial for the levelised cost of methanol, despite a slight increase in CAPEX due to lower OPEX. Using the validated process model for grey methanol, green methanol was modelled, replacing the syngas feed with a 75/25 mixture of hydrogen and carbon dioxide. For a base, case the CAPEX model was compared to literature data for green methanol plants at varying production capacities. Despite significant scatter in the data, the implemented CAPEX model captures the trend in the data well, also CAPEX curves factoring in economy of scale. A Kriging surrogate model, based on the green methanol simulation, was trained and validated and used for optimisation with the following independent variables: purge rate, reactor loop feed pressure, reactor temperature (on the boiling water side), and reactor catalyst volume (number of reactor tubes). Optimisation using the surrogate model and different optimisers showed similar performance of the SLSQP and SHGO algorithms. Since the latter is a global optimiser further optimisations for optimal parameter settings ware carried out with the SHGO algorithm for minimum CAPEX, minimum OPEX, minimum power requirement, maximum methanol production and minimum levelised cost. Different opbjectives led to different optimal solutions. Especially the solutions for minimum power and maximum methanol production were furthest apart. The latter requiring the highest pressure and temperature and the former the lowest pressure and the highest reactor volume. The minimum levelised cost is found at a reactor loop feed pressure of 78.5 bar, a boiling water temperature in the reactor of 253°C, a purge rate at the minimum applied bound, and reactor catalyst volume approx. twice that for grey methanol synthesis at the same production rate. Apparently, green methanol seems to

benefit from slightly milder conditions in the reactor both in terms of pressure and temperature, and the purge rate is of pivotal importance due to the high cost of green hydrogen. Using a multi-objective global optimisation algortithm (NSGA-II), it was also demonstrated that using the levelised cost of methanol as single objective was close to a pareto optimal solution for three objectives: minimum CAPEX, minimum power and maximum methanol production.

Acknowledgement

The authors acknowledge language secretary Susanne Tolstrup, Safety department, Ramboll Energy Transition for proofreading this manuscript. Numerous discussions with colleagues has also contributed to the making of this manuscript. Hugo Silva, Kim Pilgaard, Sten Petterson from the Process Department of Ramboll Energy Transion. From Department of Chemical and Biochemical Engineering, Technical University, Professor Gürkan Sin and research assistant Pierre Guilloteau is also acknowledged for numerous fruitful discussions.

References

(1) Ott, J.; Gronemann, V.; Pontzen, F.; Fiedler, E.; Grossmann, G.; Kersebohm, D. B.; Weiss, G.; Witte, C. *Ullmann's Encyclopedia of Industrial Chemistry*; John Wiley & Sons, Ltd, 2012.

(2) Nestler, F.; Krüger, M.; Full, J.; Hadrich, M. J.; White, R. J.; Schaadt, A. Methanol Synthesis, Industrial Challenges within a Changing Raw Material Landscape. *Chemie Ingenieur Technik* **2018**, *90*, 1409–1418.

(3) Bowker, M. Methanol Synthesis from CO2 Hydrogenation. *ChemCatChem* **2019**, *11*, 4238–4246.

(4) Roode-Gutzmer, Q. I.; Kaiser, D.; Bertau, M. Renewable Methanol Synthesis. *ChemBioEng Reviews* **2019**, *6*, 209–236.

(5) Dieterich, V.; Buttler, A.; Hanel, A.; Spliethoff, H.; Fendt, S. Power-to-liquid via synthesis of methanol, DME or Fischer–Tropsch-fuels: a review. *Energy Environ. Sci.* **2020**, *13*, 3207–3252, Publisher: The Royal Society of Chemistry.

(6) Beck, A.; Newton, M. A.; van de Water, L. G. A.; van Bokhoven, J. A. The Enigma of Methanol Synthesis by Cu/ZnO/Al2O3-Based Catalysts. *Chemical Reviews* **2024**, *124*, 4543–4678.

(7) Atsbha, T. A.; Yoon, T.; Yoo, B.-H.; Lee, C.-J. Techno-Economic and Environmental Analysis for Direct Catalytic Conversion of CO2 to Methanol and Liquid/High-Calorie-SNG Fuels. *Catalysts* **2021**, *11*.

(8) Lacerda de Oliveira Campos, B.; John, K.; Beeskow, P.; Herrera Delgado, K.; Pitter, S.; Dahmen, N.; Sauer, J. A Detailed Process and Techno-Economic Analysis of Methanol Synthesis from H2 and CO2 with Intermediate Condensation Steps. *Processes* **2022**, *10*.

(9) Cameli, F.; Delikonstantis, E.; Kourou, A.; Rosa, V.; Van Geem, K. M.; Stefanidis, G. D. Conceptual Process Design and Technoeconomic Analysis of an e-Methanol Plant with Direct Air-Captured CO2 and Electrolytic H2. *Energy & Fuels* **2024**, *38*, 3251–3261.

(10) Luyben, W. L. Design and Control of a Methanol Reactor/Column Process. *Industrial & Engineering Chemistry Research* **2010**, *49*, 6150–6163, Publisher: American Chemical Society.

(11) Alarifi, A.; Alsobhi, S.; Elkamel, A.; Croiset, E. Multiobjective Optimization of Methanol Synthesis Loop from Synthesis Gas via a Multibed Adiabatic Reactor with Additional Interstage CO2 Quenching. *Energy & Fuels* **2015**, *29*, 530–537.

(12) Bussche, K. M. V.; Froment, G. F. A Steady-State Kinetic Model for Methanol Synthesis and the Water Gas Shift Reaction on a Commercial Cu/ZnO/Al2O3Catalyst. *Journal of Catalysis* **1996**, *161*, 1–10.

(13) Van-Dal, S.; Bouallou, C. Design and simulation of a methanol production plant from CO2 hydrogenation. *Journal of Cleaner Production* **2013**, *57*, 38–45.

(14) Mignard, D.; Pritchard, C. On the use of electrolytic hydrogen from variable renewable energies for the enhanced conversion of biomass to fuels. *Chemical Engineering Research and Design* **2008**, *86*, 473–487.

(15) Miranda, J.; Ponce, G.; Arellano-Garcia, H.; Maciel Filho, R.; Wolf Maciel, M. Syngas to Higher Alcohols Using Cu-Based Catalyst - A Simulation Approach. *Chemical Engineering Transactions* **2015**, *43*, 1519–1524.

(16) Chiang, C.-L.; Lin, K.-S. Preparation and characterization of CuOAl2O3 catalyst for dimethyl ether production via methanol dehydration. *International Journal of Hydrogen Energy* **2017**, *42*, 23526–23538.

(17) van Baten, J. COCO - the CAPE-OPEN to CAPE-OPEN simulator. `https://www.cocosimulator.org/index.html`.

(18) ChemSep: Program - Overview. `http://www.chemsep.org/`.

(19) The CAPE-OPEN Laboratories Network. 2024; `https://www.colan.org/`.

(20) van Baten, J.; Pons, M. CAPE-OPEN: Interoperability in Industrial Flowsheet Simulation Software. *Chemie Ingenieur Technik* **2014**, *86*, 1052–1064.

(21) Peng, D.-Y.; Robinson, D. B. A New Two-Constant Equation of State. *Industrial & Engineering Chemistry Fundamentals* **1976**, *15*, 59–64.

(22) Taylor, R.; Kooijman, H. *The ChemSep Book*; Books on Demand, 2001.

(23) KDB (Korea Thermophysical Properties Data Bank). https://www.cheric.org/research/kdb/.

(24) de Medeiros, D. W. O. DWSIM - the open source process simulator. 2024; https://dwsim.org/.

(25) Woods, D. R. *Rules of Thumb in Engineering Practice*; John Wiley & Sons, Ltd, 2007; Chapter Appendix D: Capital Cost Guidelines, pp 376–436.

(26) van Amsterdam, M. Factorial Techniques applied in Chemical Plant Cost Estimation. Ph.D. thesis, Delft University of Technology, 2018.

(27) Jensen, E. H.; Andreasen, A.; Jørsboe, J. K.; Andersen, M. P.; Hostrup, M.; Elmegaard, B.; Riber, C.; Fosbøl, P. L. Electrification of amine-based CO2 capture utilizing heat pumps. *Carbon Capture Science & Technology* **2024**, *10*, 100154.

(28) Cakartas, M.; Zhou, J.; Ren, J.; Andreasen, A.; Yu, H. In *34th European Symposium on Computer Aided Process Engineering / 15th International Symposium on Process Systems Engineering*; Manenti, F., Reklaitis, G. V., Eds.; Computer Aided Chemical Engineering; Elsevier, 2024; Vol. 53; pp 2077–2082.

(29) Short, W.; Packey, D. J.; Holt, T. *A Manual for the Economic Evaluation of Energy Efficiency and Renewable Energy Technologies NREL/TP-462-5173*; 1995.

(30) Peters, M. S.; Timmerhaus, K. D. *Plant design and economics for chemical engineers*, 5th ed.; McGraw Hill: New Delhi, 2003.

(31) Towler, G.; Sinnott, R. *Chemical Engineering Design (Second Edition)*, second edition ed.; Butterworth-Heinemann: Boston, 2013; pp 3–32.

(32) Seider, W.; Lewin, D.; Seader, J.; Widagdo, S.; Gani, R.; Ng, K. *Product and Process Design Principles: Synthesis, Analysis and Evaluation*; Wiley, 2016.

(33) Eblé, L.; Weeda, M. *Evaluation of the levelised cost of hydrogen based on proposed electrolyser projects in The Netherlands: Renewable Hydrogen Cost Element Evaluation Tool (RHyCEET)*; TNO Public TNO 2024 R10766, 2024.

(34) Turton, R.; Shaeiwitz, J.; Bhattacharyya, D.; Whiting, W. *Analysis, Synthesis, and Design of Chemical Processes*; Prentice-Hall international series in the physical and chemical engineering sciences; Prentice Hall, 2018.

(35) The hydrogen trajectory - KPMG. 2023; `https://kpmg.com/be/en/home/insights/2021/03/eng-the-hydrogen-trajectory.html`.

(36) European Hydrogen Observatory. 2024; `https://observatory.clean-hydrogen.europa.eu/`.

(37) Kearns, D.; Liu, H.; Consoli, C. *Technology readiness and costs of CCS*; 2021.

(38) Andreasen, A. Applied Process Simulation-Driven Oil and Gas Separation Plant Optimization Using Surrogate Modeling and Evolutionary Algorithms. *ChemEngineering* **2020**, *4*.

(39) Aspelund, A.; Gundersen, T.; Myklebust, J.; Nowak, M.; Tomasgard, A. An optimization-simulation model for a simple LNG process. *Computers & Chemical Engineering* **2010**, *34*, 1606 – 1617.

(40) Caballero, J. A.; Grossmann, I. E. An algorithm for the use of surrogate models in modular flowsheet optimization. *AIChE Journal* **2008**, *54*, 2633–2650.

(41) Olsen, E.; Hooghoudt, J.-O.; Maschietti, M.; Andreasen, A. Optimization of an Oil and Gas Separation Plant for Different Reservoir Fluids using an Evolutionary Algorithm. *Energy Fuels* **2021**, *35*, 5392—-5406.

(42) Kim, I. H.; Dan, S.; Kim, H.; Rim, H. R.; Lee, J. M.; Yoon, E. S. Simulation-Based

Optimization of Multistage Separation Process in Offshore Oil and Gas Production Facilities. *Industrial & Engineering Chemistry Research* **2014**, *53*.

(43) Box, G.; Hunter, W.; Hunter, J. *Statistics for Experimenters*; John Wiley & Sons, 1978.

(44) Myers, R. H.; Montgomery, D. C.; Anderson-Cook, C. M. *Response Surface Methodology*; John Wiley & Sons, 2009.

(45) Faraway, J. J. *Linear Models with R*; Chapman and Hall/CRC, 2004.

(46) Kraft, D. Algorithm 733: TOMP–Fortran Modules for Optimal Control Calculations. *ACM Trans. Math. Softw.* **1994**, *20*, 262–281.

(47) Mckay, M. D.; Beckman, R. J.; Conover, W. J. A Comparison of Three Methods for Selecting Values of Input Variables in the Analysis of Output from a Computer Code. *Technometrics* **2000**, *42*, 55–61.

(48) Morris, M. D.; Mitchell, T. J. Exploratory designs for computational experiments. *Journal of Statistical Planning and Inference* **1995**, *43*, 381 – 402.

(49) Paulson, C.; Ragkousis, G. pyKriging: A Python Kriging Toolkit. 2015; `https://doi.org/10.5281/zenodo.21389`.

(50) Loeppky, J. L.; Sacks, J.; Welch, W. J. Choosing the Sample Size of a Computer Experiment: A Practical Guide. *Technometrics* **2009**, *51*, 366–376.

(51) Afzal, A.; Kim, K.-Y.; won Seo, J. Effects of Latin hypercube sampling on surrogate modeling and optimization. *International Journal of Fluid Machinery and Systems* **2017**, *10*, 240–253.

(52) Krige, D. *A statitical approach to some mine valuation and allied problems on the Witwatersrand (Master thesis)*; University of the Witwatersrand, 1951.

(53) Matheron, G. Principles of geostatistics. *Economic Geology* **1963**, *58*, 1246–1266.

(54) Jones, D. R. A Taxonomy of Global Optimization Methods Based on Response Surfaces. *Journal of Global Optimization* **2001**, *21*, 345–383.

(55) Ragkousis, G. E.; Curzen, N.; Bressloff, N. W. Multi-objective optimisation of stent dilation strategy in a patient-specific coronary artery via computational and surrogate modelling. *Journal of Biomechanics* **2016**, *49*, 205 – 215.

(56) Paulson, C. The rapid development of bespoke sensorcraft : a proposed design loop for small unmanned aircraft. Ph.D. thesis, Faculty of Engineering and the Environment Computational Engineering and Design Group, University of Southhampton, 2017.

(57) Davis, E.; Ierapetritou, M. A kriging method for the solution of nonlinear programs with black-box functions. *AIChE Journal* **2007**, *53*, 2001–2012.

(58) Quirante, N.; Javaloyes, J.; Ruiz-Femenia, R.; Caballero, J. A. In *12th International Symposium on Process Systems Engineering and 25th European Symposium on Computer Aided Process Engineering*; Gernaey, K. V., Huusom, J. K., Gani, R., Eds.; Computer Aided Chemical Engineering; Elsevier, 2015; Vol. 37; pp 179 – 184.

(59) Klier, K.; Chatikavanij, V.; Herman, R.; Simmons, G. Catalytic synthesis of methanol from COH2: IV. The effects of carbon dioxide. *Journal of Catalysis* **1982**, *74*, 343–360.

(60) Andreasen, A.; Rasmussen, K. R.; Mandø, M. Plant Wide Oil and Gas Separation Plant Optimisation using Response Surface Methodology. *IFAC-PapersOnLine* **2018**, *51*, 178 – 184, 3rd IFAC Workshop on Automatic Control in Offshore Oil and Gas Production OOGP 2018.

(61) Vaquerizo, L.; Kiss, A. A. Thermally self-sufficient process for cleaner production of e-methanol by CO2 hydrogenation. *Journal of Cleaner Production* **2023**, *433*, 139845.

(62) Pérez-Fortes, M.; Schöneberger, J. C.; Boulamanti, A.; Tzimas, E. Methanol synthesis

using captured CO2 as raw material: Techno-economic and environmental assessment. *Applied Energy* **2016**, *161*, 718–732.

(63) Cordero-Lanzac, T.; Ramirez, A.; Navajas, A.; Gevers, L.; Brunialti, S.; Gandía, L. M.; Aguayo, A. T.; Mani Sarathy, S.; Gascon, J. A techno-economic and life cycle assessment for the production of green methanol from CO2: catalyst and process bottlenecks. *Journal of Energy Chemistry* **2022**, *68*, 255–266.

(64) Nyári, J.; Magdeldin, M.; Larmi, M.; Järvinen, M.; Santasalo-Aarnio, A. Techno-economic barriers of an industrial-scale methanol CCU-plant. *Journal of CO2 Utilization* **2020**, *39*, 101166.

(65) Mucci, S.; Mitsos, A.; Bongartz, D. Cost-optimal Power-to-Methanol: Flexible operation or intermediate storage? *Journal of Energy Storage* **2023**, *72*, 108614.

(66) Virtanen, P. et al. SciPy 1.0: Fundamental Algorithms for Scientific Computing in Python. *Nature Methods* **2020**, *17*, 261–272.

(67) Deb, K.; Pratap, A.; Agarwal, S.; Meyarivan, T. A fast and elitist multiobjective genetic algorithm: NSGA-II. *IEEE Transactions on Evolutionary Computation* **2002**, *6*, 182–197.

(68) Hadka, D. Platypus - A Free and Open Source Python Library for Multiobjective Optimization. 2024; `https://github.com/Project-Platypus/Platypus`.

TOC Graphic